BRIGHTON, 13 - 16.9.1993
EPE

FREQUENCY DOMAIN MODELLING OF TRACTION PWM CONVERTERS

J A Taufiq and J Shen

GEC ALSTHOM Traction Ltd., UK.

Abstract. In a previous paper by one of the authors (1), a frequency domain model (FDM) was described for calculating the DC side harmonics in a traction VSI drive. In this paper, this principle has been extended to describe a FDM for an interlaced PWM converter drive system. Such a model, which can be 20–30 times faster than the corresponding time domain model, is useful for obtaining steady-state results of these drives for systems engineering. Typical results which can be produced are circuit and device waveforms, harmonic spectra and psophometric current. Such a fast simulation tool is particularly invaluable when a series of calculations are required over the entire speed range of the designed drive system. Results from an interlaced PWM converter fed inverter drive simulation are presented, including the effects of parameter asymmetry and load unbalance. A comparison is also made of the computed converter input current waveforms and those measured from a 1.5MVA test rig. Computed and measured converter input current harmonic spectra are also compared to confirm the accuracy of the FDM.

Keywords. Circuit simulation, PWM converter, traction

LIST OF SYMBOLS USED

V_P,	V_S	Transformer primary and secondary voltages (rms)
I_S		Transformer secondary current (rms)
V_C		Converter input voltage (rms)
SV_C		Switching function equivalent to V_C of amplitude $\pm$ 1
V_L		Voltage across transformer secondary inductance (rms)
ϕ		Phase shift between V_C and V_S
I_O		Converter output current
I_F		Second harmonic filter current
V_D,	I_D	DC link voltage and current
L_s		Transformer secondary inductance
L_f,	C_f	Second harmonic filter components
C_d		DC link capacitance
P_S,	Q_S	Transformer secondary active and reactive powers
P_C,	Q_C	Converter input active and reactive powers
M_I,	M_R	Modulation index and ratio
$I_O(n)$		n^{th} harmonic amplitude of I_O
t_q,	t_d	GTO turn-off and delay times

INTRODUCTION

The Frequency Domain Model (FDM) which is used for steady state analysis involves decomposing a circuit switching waveform into its harmonics and applying these individually to an equivalent circuit in order to compute the corresponding current harmonics. These can then be used to calculate signalling related current harmonics, or summed vectorially to construct various circuit and device waveforms. In the case of a Voltage Source Inverter (VSI), it has been shown by Taufiq and Xiaoping (1) that by only using selected pairs of switching waveform harmonics, accurate current harmonics and waveforms can be obtained. This leads to a saving in computation time as only a limited number of spectral multiplications are performed. Also the FDM can be 20–30 times faster than the corresponding time domain PWM converter model such as described by Schlunegger (2). However, the FDM cannot easily be used for transient analysis as would be required for control system design. In such cases the time domain model is required.

Circuit Relationships

The closed-loop operation of the PWM converter ensures unity displacement factor operation at the transformer secondary. For this condition, and assuming that the transformer secondary inductance has no resistive component, the active and reactive power components for motoring at the transformer secondary and converter input are given by,

$$\left.\begin{aligned} P_S &= V_S I_S,\ \ Q_S = 0 \\ P_C &= V_S I_S,\ \ Q_C = -\frac{V_L{}^2}{\omega L_s} \end{aligned}\right\}\ \textit{for motoring} \qquad (1)$$

Eqn (1) shows that the impedance at the converter input will have a varying resistive component (for P_C) in parallel with a varying capacitance (for Q_C). This capacitance will be such that there is reactive power balance with L_s. This will result in a purely resistive input impedance at the transformer secondary, thus giving unity displacement factor operation.

Assuming a lossless PWM converter, then from Fig 1, $V_C(t)I_S(t)$ must be equal to $I_O(t)V_D(t)$. If there is no DC link voltage ripple, then $I_O(t)$ will be given by,

$$I_O(t) = \frac{V_C I_S}{V_D}[\cos\phi - \cos(2\omega t - \phi)] \qquad (2)$$

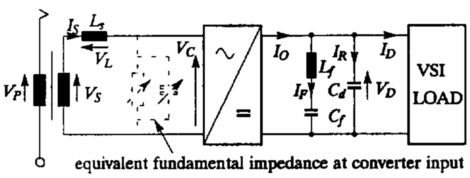

Fig. 1 Block diagram of single PWM converter

Eqn (2) shows that $I_O(t)$ contains a DC component $I_O(0)$ of amplitude $V_C I_S \cos\phi / V_D$ and a second harmonic component $I_O(2)$ of amplitude $V_C I_S / V_D$. These components can also be shown to be given by,

$$I_O(0) = \frac{V_S I_S}{V_D},\ I_O(2) = \frac{M_f I_S}{\sqrt{2}},\ I_O(0) < I_O(2) \qquad (3)$$

$I_O(2)$ will mainly flow in the second harmonic filter consisting of L_f, C_f thus limiting the second harmonic voltage ripple in V_D. It is crucial to reduce the resistance of this filter for this reason. The current in this filter, I_F, will therefore consist largely of $I_O(2)$ together with some ripple associated with the PWM action of the converter and VSI.

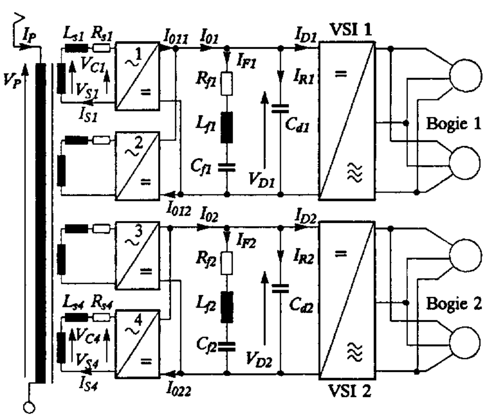

Fig. 2 PWM converter drive system simulated

SYSTEM MODELLED

The system simulated is shown in Fig 2 and consists of four interlaced PWM converters feeding two VSIs. The carrier waveform phase shifts for converters 1–4 are 0°, 90°, 45°, 135° respectively so that interlaced operation is still maintained under a bogie cut out condition. In general, for n interlaced converters, the carrier phase shift required is given by 180°/n. A closed-loop control system based on the well known phasor diagram control scheme is used.

The FDM for the VSI is that described in (1) and ideal switching characteristics are assumed for the circuit GTOs and diodes. This assumption also applies for the PWM converter model. However, it is possible to include the effect of the GTO turn-off time t_q and delay time t_d in the VSI and PWM converter. The effect of these times on the harmonics of I_S can thus be studied.

With reference to Fig 2, given below are the mathematical models for the various parts of the circuit. The second harmonic of $\overline{I_{F1}}$ is calculated from Eqn (4) based on the impedance ratio of the filter and the DC link capacitor.

$$\overline{I_{F1}}(2) = \frac{\overline{I_{O1}}(2)}{(1 + j200\pi C_{d1} R_{f1})} \qquad (4)$$

The DC link capacitor current harmonics are given by Eqn (5)

$$\overline{I_{R1}}(n) = \overline{I_{O1}}(n) - \overline{I_{F1}}(n) - \overline{I_{D1}}(n) \qquad (5)$$

The transformer secondary currents are computed from Eqn (6). The voltage difference between $\overline{V_S}$ and $\overline{V_C}$ is applied to a first order lag and the corresponding current components are summed vectorially to construct $\overline{I_S}$.

$$\overline{I_{S1}} = \sum_{n=1}^{m} \frac{\overline{V_{S1}}(n) - \overline{V_{C1}}(n)}{(R_{s1} + jn\omega L_{s1})} \qquad (6)$$

Clearly, if $\overline{V_S}$ is assumed to be sinusoidal, the computation of the harmonics in Eqn (6) is simplified.

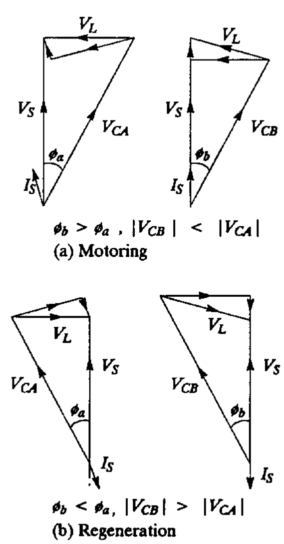

Fig. 3 Phasor diagrams with the resistive component of L_s ignored and included

Fig 3 shows the phasor diagram in motoring and braking for the cases when the resistance of L_s is ignored and included. With this term ignored in motoring, I_S will tend to assume a leading phase angle which can typically be around +5°. The amplitude and phase shift of $\overline{V_C}$ is given by Eqn (7).

$$|V_{C1}(1)| = \sqrt{[I_{S1}(1)\omega L_{s1}]^2 + [V_{S1}(1) \pm I_{S1}(1)R_{s1}]^2}$$

$$\phi = \pm \cos^{-1}\frac{[V_{S1}(1) \pm I_{S1}(1)R_{s1}]}{V_{C1}(1)} \qquad (7)$$

+ : regeneration; - : motoring

The PWM waveform corresponding to $\overline{V_{C1}}$ is then constructed depending on the type of PWM scheme adopted for the PWM converter. The corresponding value of M_I is given by Eqn (8).

$$M_I = \frac{\sqrt{2}V_{C1}}{V_D} \qquad (8)$$

Unlike a VSI the value of M_I in a PWM converter only varies over a relatively narrow range of values. From Fig 3 the minimum value occurs at no-load when V_C is equal to V_S. The maximum value occurs when the minium pulse-width limit T_{min} of the PWM waveform is reached. These two extreme values can be shown to be given by Eqn (9), where f_c is the PWM carrier frequency. T_{min} is typically 100–150 μs for a traction PWM converter and the range of M_I is usually $0.95 > M_I > 0.7$.

$$M_{I_{\min}} = \frac{\sqrt{2}V_S}{V_D}, M_{I_{\max}} = 1 - 2f_cT_{\min} \qquad (9)$$

The individual converter output current (e.g. I_{O11}) can be obtained from I_S and SV_C, the switching function equivalent to V_C, by using Eqn (10).

Having computed I_{O11} to I_{O22}, the two currents I_{O1} and I_{O2} are computed by vectorial addition. This completes the description of the FDM used for the PWM converter.

$$\overline{I_{O11}} = \overline{I_{S1}} \cdot \overline{SV_{C1}} \qquad (10)$$

RESULTS

Fig 4 shows some typical DC side waveforms produced with the FDM in motoring. The simulation data is as given in Table 1. The large second harmonic component in I_{O1} can be clearly seen. Similarly, the waveforms in regeneration can also be produced with the model. In order to validate the FDM a comparison was made with the measured current waveforms from a high power PWM converter test rig. This comparison is shown in Fig 5. The accuracy of the model is confirmed by the close agreement between the two sets of waveform. By multiplying the computed $\overline{I_{S1}}$ and the corresponding logic switching function for each pole (or leg) of the PWM converter bridge, the respective device switching waveforms can be obtained. These are useful in determining junction, pole face and heatsink temperature rises, for a given duty cycle of the PWM converter. The very short execution time of the FDM means that numerous device current computations can be performed for a given station to station run (which may be in the order of 10 mins or more) thus improving the accuracy of the thermal model.

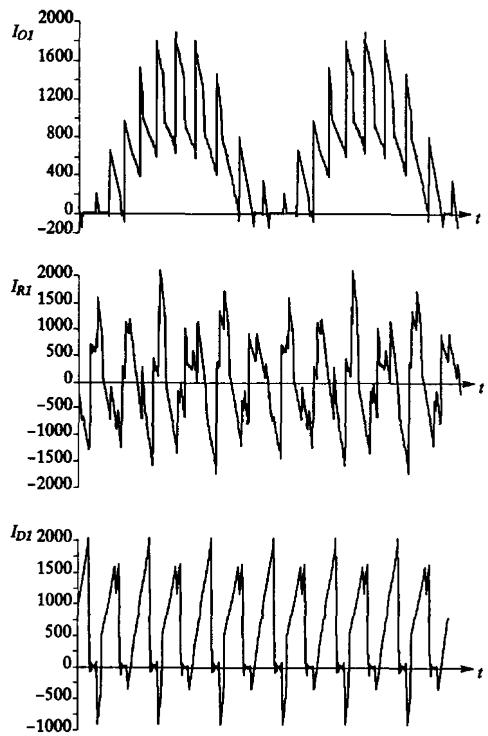

Fig. 4 Typical DC side waveforms produced by the FDM in motoring

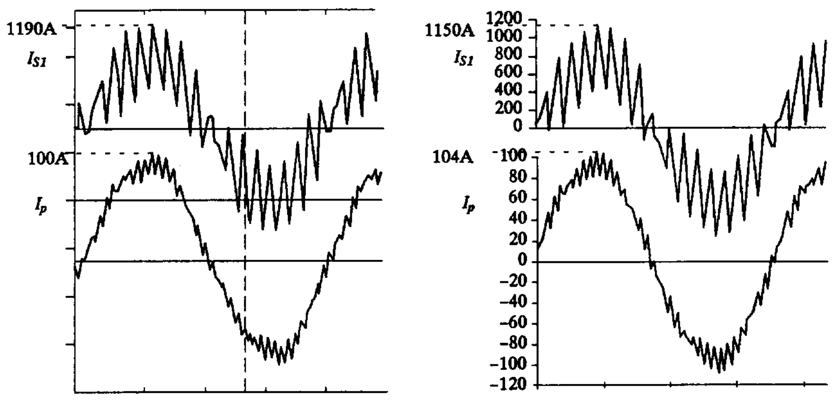

(a) Measured (b) Computed

Fig. 5 Comparison between measured and computed waveforms (2 interlaced PWM converters, M_R = 9, 1.3MW load)

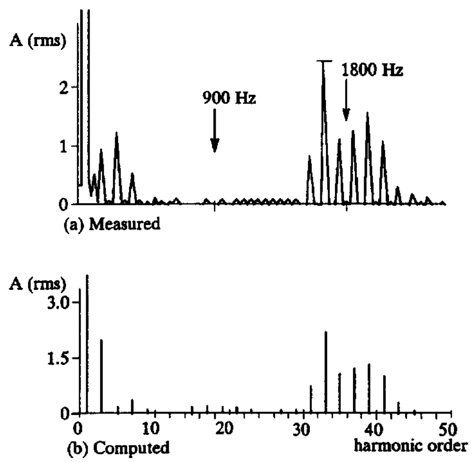

Fig. 6 Comparison between measured and computed harmonic spectra of I_p (M_R = 9)

Fig 6 shows the comparison between the computed and measured harmonic spectra of I_P for the results in Fig 5. Since there are two interlaced PWM converters each with M_R = 9, the main harmonics of I_P occur on either side of $4M_Rf$, where f is the fundamental frequency. Since f = 50Hz in this case, these harmonics are centred around 1800Hz. From Fig 6 the correlation between the amplitudes of these harmonics is good. The harmonic spectrum of the individual secondary currents will contain components centred around $2M_Rf$ and multiples of it. Due to the interlaced operation, the components centred around odd multiples of $2M_Rf$ do not appear in the spectrum of I_P for two interlaced PWM converters. Similarly, for four interlaced PWM converters, the harmonics of I_P will be centred around $8M_Rf$ and multiples of it. The fundamental component in Fig 6 has been deliberately suppressed in order to show clearly the amplitude of these harmonics. Several low order harmonics, notably the 3rd, 5th, 7th and 9th can also be seen in the two spectra. The correlation for these is not as good. The amplitudes of these harmonics are affected by t_d, t_q and also the DC link voltage ripple. These effects were not included in the FDM from which the computed spectrum was produced.

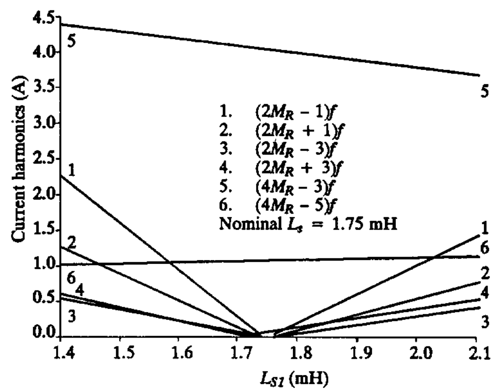

Fig. 7 Harmonics introduced by differences in L_s for two interlaced PWM converters

Unbalance Effects

With interlaced PWM converter operation, we have so far assumed that the individual transformer secondary inductances are identical in value. In practice this inductance will be incorporated into the transformer leakage inductance and can vary slightly from one secondary to another, depending on the transformer manufacturing tolerances. Each group of two interlaced PWM converters in Fig 2 will have a common closed-loop controller with only the PWM waveform generation being different for the two converters. Any variation in L_s will have the effect of introducing in I_P harmonics which would otherwise have been cancelled through interlacing. Fig 7 shows the variation in the $2M_R \pm n$ group of harmonics for up to a ± 20% change in one of the L_s values in the case of two interlaced PWM converters. In this case such a parameter unbalance will also result in a load unbalance between the two converters. Fig 7 also shows that the harmonics centred around $4M_Rf$, which are present in I_P anyway, are not really affected by this degree of unbalance. Fig 8 shows the case for four interlaced PWM converters with $L_{s1} = L_{s2}$ and $L_{s3} = L_{s4}$ but with up to a ± 20% difference in value between the two groups. In this case it will be normal to have independent closed-loop control for the two groups of converters. Therefore, unlike the previous case, there will be no power unbalance between the four converters provided that the two DC link loads are the same. However, the ripple in I_{S1} and I_{S3} will be different due to the difference in L_s. In this case the variation in the $4M_R \pm n$ group of harmonics is shown in Fig 8. For all cases the simulation data is given in Table 1.

Fig 9 shows the effect on the harmonics of I_P of a power unbalance between the two groups of PWM converters resulting from different power levels for the two bogies. Such an effect can be encountered with differences in wheel diameters between bogies. Here L_{s1} - L_{s4} have been taken to be identical and two independent controllers for the two groups of converters assumed.

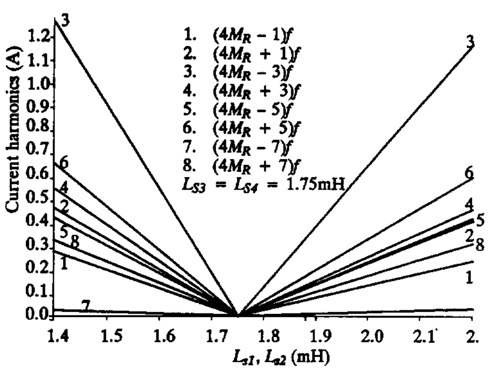

Fig. 8 Harmonics introduced by differences in L_s for four interlaced PWM converters ($L_{s1} = L_{s2}, L_{s3} = L_{s4}$)

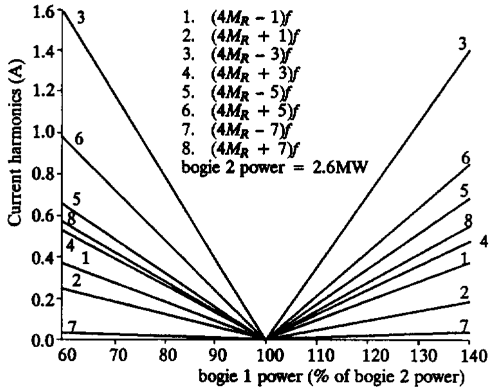

Fig. 9 Harmonics produced by power unbalance between two groups of four interlaced PWM converters

CONCLUSIONS

The FDM for the PWM converter described in this paper has been found to be a valuable tool for systems engineering design of such equipment. Although only limited to steady-state analysis, the model has extensive use for the computation of circuit waveforms, signalling harmonics and psophometric current. The model described in this paper is for interlaced two level PWM converters. This model can also be used for analysis of interlaced three level PWM converters.

References

1 Taufiq, J.A. & Xiaoping, J.:'Fast accurate computation of the DC side harmonics in a traction VSI drive', IEE Proc., Vol. 136, Pt. B, No. 4, July 1989, pp 176–187.

2 Schlunegger, H.:'Digital simulations of a forced-commutated converter for single phase for AC locomotives' IFAC Conf., 1977, Dusseldorf, pp 759–767.

Table 1 Main data for simulation model

V_S = 1450V, 50Hz	C_d = 6mF
P_S = 5.2MW nominal	L_f = 0.84mH
ωL_s = 0.34pu	C_f = 3mF
R_s = 13.5mΩ	R_f = 15mΩ
V_D = 2.8kV	M_R = 5

(regular asymmetric sampling)